数理解析研究所講究録
第1724巻 2011年 167-175

PARALLEL COMPUTATION OF COMPRESSIBLE MULTI-FLUID FLOW

Angel M. Bethancourt L.
Institute of Computational Fluid Dynamics
Masahiro Egami
Honda R&D, Co. Ltd.

Abstract. A collapse of a helium bubble due to its interactions with an incoming shock wave is numerically examined. The flow is modeled using the two-dimensional compressible Euler equations with an additional equation of motion for the propagating interface. The solution is obtained in a two-step manner, first, the Euler's system of equations is solved using Roe's flux difference splitting scheme; second, the moving interface (a function of the specific heat ratio is used to mark the fluids interface) is captured using a third-order WENO scheme. For both, a third-order Runge-Kutta method is used for time integration. The solver is parallelized, allowing us to conduct fine mesh computations, and enabling the numerical reproduction of the mechanisms observed in previous published experiments.

1. Introduction

Early attempts to compute multi-fluid flow, consisted in incorporating a conservative form of the advection equation for the material interface into the Euler system of equation [1,2,3], and solve them using standard methods developed for the classical Euler equations. However, it was observed that spurious oscillations develop at the material interfaces due to differences in fluid properties at the interface, as well as, errors in the location of the interface. In order to solve some of the problems, a quasi-conservative is proposed in [1], in which the advection equation is decoupled from the Euler equations and written in non-conservative form.

Additional modifications to the governing equations are made in [4,5], which render the algorithm "single-fluid" when calculating the interface fluxes at the expense of conservation, to improve the coupling of the advection-Euler equations and to account for pressure equilibrium across the interface.

In this paper, the quasi-conservative method described in [1,4] is implemented. Because our interest is on high-resolution computations, this implementation is extended using MPI (Message Passing Interface) libraries for its parallelization. As application, the interactions between a helium bubble and a Mach 1.22 shock wave in air is studied.

2. Equations of motion

For the problem at hand, we limit our analysis to two immiscible ideal gases, $p=(\gamma-1)\rho e$, characterized by their constant ratio of specific heats, γ. The two-dimensional Euler equations for such multi-component flow in conservative form are

$$\frac{\partial Q}{\partial t}+\frac{\partial E}{\partial x}+\frac{\partial F}{\partial y}=0, \tag{1}$$

$$Q=\begin{bmatrix}\rho\\ \rho u\\ \rho v\\ e\end{bmatrix};\ E=\begin{bmatrix}\rho u\\ \rho u^2+p\\ \rho uv\\ (e+p)u\end{bmatrix};\ F=\begin{bmatrix}\rho v\\ \rho uv\\ \rho v^2+p\\ (e+p)v\end{bmatrix}$$

where ρ is the density, u and v are the velocity components, p is the pressure, and e is the total energy of the fluid.

The moving interface is captured using the discontinuity in the ratio of the specific heats for the different components. Since material interfaces are advected by the flow, any function of γ obeys the advection equation [1],

$$\frac{\partial f(\gamma)}{\partial t}+u\frac{\partial f(\gamma)}{\partial x}+v\frac{\partial f(\gamma)}{\partial y}=0, \quad \therefore\ f(\gamma)=\frac{1}{\gamma-1} \tag{2}$$

Spatial discretization of (1) is done using Roe's flux difference splitting scheme. The numerical flux is given by:

$$E_{i+1/2}=E(Q_L,Q_R)=\frac{1}{2}\left[E(Q_L)+E(Q_R)\right]-\frac{1}{2}|A|\left[Q_R-Q_L\right], \text{ where } A=\frac{\partial E}{\partial Q} \tag{3}$$

A is the Jacobian matrix based on Roe's average of Q_L and Q_R. The modification introduced in [4] consists in calculating two fluxes at the cell interface, by "freezing" the values of γ in either side of the interface:

$$E^L_{i+1/2}=E(Q_L,Q_R;\gamma_L)$$
$$E^R_{i+1/2}=E(Q_L,Q_R;\gamma_R)$$

Then, use $E^L_{i+1/2}$ to update the flux in cell i and $E^R_{i+1/2}$ to update the flux in cell $i+1$.

The spatial discretization of (2) is carried out using a third-order WENO scheme [6]. A TVD third order Runge-Kutta method is used to solve both the Euler and advection equations [6]. The equations are written as, $Q_t=L(u)$, where $L(u)$ is the discretization of the spatial derivatives, and advanced in time according to the algorithm:

$$
\begin{aligned}
Q^{(1)} &= Q^n + \Delta t L(Q^n) \\
Q^{(2)} &= \frac{3}{4}Q^n + \frac{1}{4}Q^{(1)} + \frac{1}{4}\Delta t L(Q^{(1)}) \\
Q^{n+1} &= \frac{1}{3}Q^n + \frac{2}{3}Q^{(2)} + \frac{2}{3}\Delta t L(Q^{(2)})
\end{aligned}
\tag{4}
$$

The parallelization of the code is achieved by using Domain Decomposition in conjunction with a SPMD (Single Program Multiple Data) technique. The MPI libraries are used to communicate between the different processors. Our system consists of 8 nodes, each node contains of 2cpu-IntelXeon (8 cores). The maximum number of cores available is 64.

3. Problem Definition

Our focus is on the dynamics of the interaction of a Mach 1.22 shock and a helium bubble, as presented in [7,8]. The initial conditions for this problem are given in Fig. 1, the upper and lower boundaries are considered solid walls, the inflow is from the right and properties are specified, at outflow (left) a zero gradient is imposed. A uniform grid with spatial resolution of 0.05 mm is used for the present computation, resulting in a grid size of 7121x1781. It takes approximately 12hr30min to obtain a 528 μs sample (time step: 3.3333×10^{-8}s) using 32 processors.

4. Computational Results

Figure 2 shows a sequence of idealized Schlieren images [8], showing the overall wave structure. At 24 μs, Figure 2a shows a refracted shock inside of the bubble, moving faster than incident shock, since the helium has a higher sound speed than the air. Upstream of the bubble, a reflected wave is shown moving away from the bubble. At 36 μs, Figure 2b shows a four-shock configuration which it is usually termed twin regular reflection-refraction (TRR), also shown in Figure 3. At 48 μs, Figure 2c shows the refracted wave emerging from the bubble and becoming the transmitted wave, also two cusps appear in the left-side of the bubble indicating internally reflected waves that converge toward the axis of the bubble (Figure 2d, 56 μs). At 64 μs, Figure 2e shows the internal reflected waves diverging after crossing, and the two branches of the transmitted shock cross downstream of the bubble. At 88 μs, Figure 2f the initial reflected shock has reflected from the upper and bottom walls. At larger times (228 μs), Figures 2g shows that the bubble has further deformed into a kidney shaped object. Finally, Figures 2h and 2i show an induced jet of air along the axis of the bubble, resulting in the development of two vortical structures.

Figure 3 shows the enlargement of the twin regular reflection-refraction (TRR) shock configuration as well as the locations used to compare the shock waves velocities. Table 1

shows the comparison of the present computation wave velocities with the experiment of Hass and Sturtevant [7] and Quick and Karni [8] computation. Overall agreement is excellent, except for the values of the reflected and upstream velocities; this disagreement is due to the existence of bubble contamination which affects the values of its physical properties.

Figure 4 uses the density, vorticity and density gradient function to visualize the flow. Clearly, the bulk of the vorticity is produced along the bubble interface [9], following the progress of the refracted shock inside the bubble. This is consistent with the source term ($S \equiv \frac{\nabla\rho \times \nabla p}{\rho^2}$) appearing in vorticity equation of an inviscid fluid. The motion produced by the generation of vorticity is the driven force inducing the jet along the axis of the bubble.

5. Conclusions

The goal of simulating high resolution compressible multi-fluid flow was achieved. A quasi-conservative method is successfully implemented in a parallel environment to model the interactions between a helium bubble and a shock wave. The main features of the flow are captured, and compare quite well with previous numerical and experimental results.

Further investigation will be aimed to consider flows with more stiff conditions.

References

[1] Abgrall, R., 1996 How to Prevent Pressure Oscillations in Multicomponent Flow Calculations: A Quasi Conservative Approach, *J. Comp. Phys.* **125**, 150-160

[2] Larrouturou, B., 1991, How to Preserve the Mass Fractions Positivity when Computing Compressible Multi-Component Flows, *J. Comp. Phys.* **95**, 59-84

[3] Mulder, W., Osher, S., and Sethian, J.A., 1992, Computing Interface Motion in Compressible Gas Dynamics, *J. Comp. Phys.* **100**, 209-228

[4] Abgrall, R., and Karni, S., 2001, Computations of Compressible Multifluids, *J. Comp. Phys.* **169**, 594-623

[5] Fedkiw, R.P., Aslam, T., Berriman, B., and Osher, S., 1999, A non-oscillatory Eulerian approach to interfaces in multimaterial flows (the Ghost Fluid Method), *J. Comp. Phys.* **152**, 457-492

[6] Shu, C.W., 1997, Essentially Non-Oscillatory and Weighted Essentially Non-Oscillatory Schemes for Hyperbolic Conservation Laws, *ICASE Report No. 97-65*

[7] Haas, J.-F., and Sturtevant, B. 1987 Interaction of weak shock waves with cylindrical and spherical gas inhomogeneities. *J.Fluid Mech.* **181**, 41-76.

[8] Quirk, J. J., and Karni, S. 1996, On the dynamics of a shock-bubble interaction *J. Fluid Mech.* **4** 129-163.

[9] Picone, J.M., and Boris, J.P., 1988, Vorticity generation by shock propagation through bubbles in a gas, *J. Fluid Mech.* **189**, 23-51

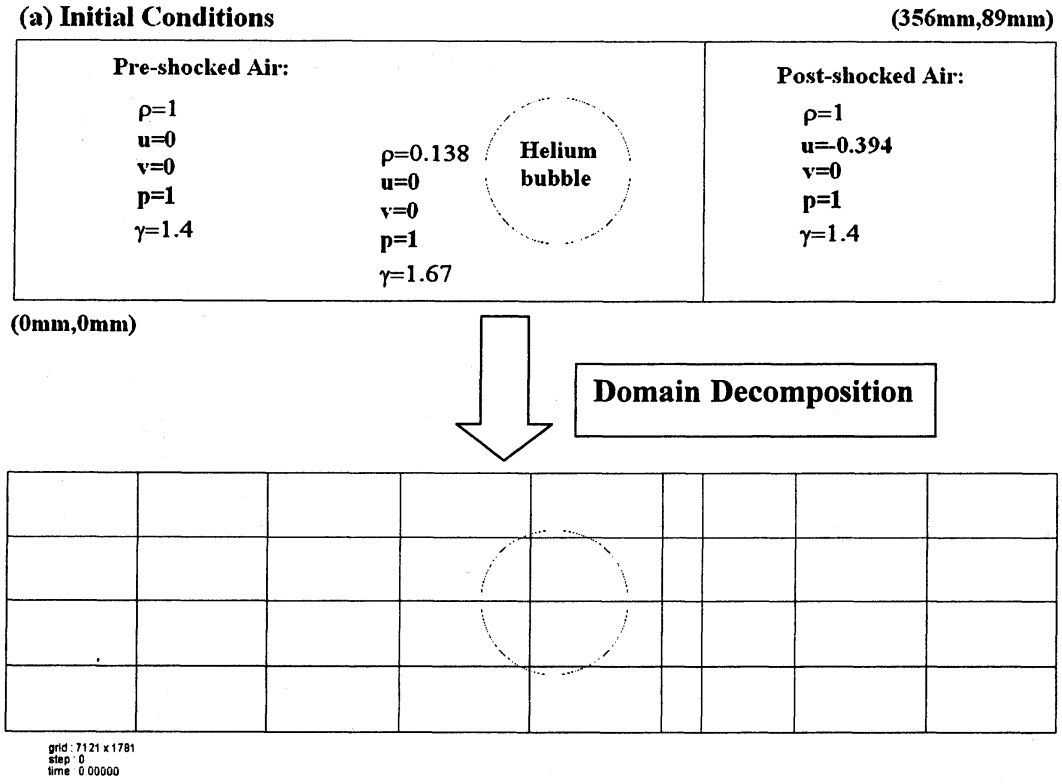

Figure 1. Computational domain and initial parameters.

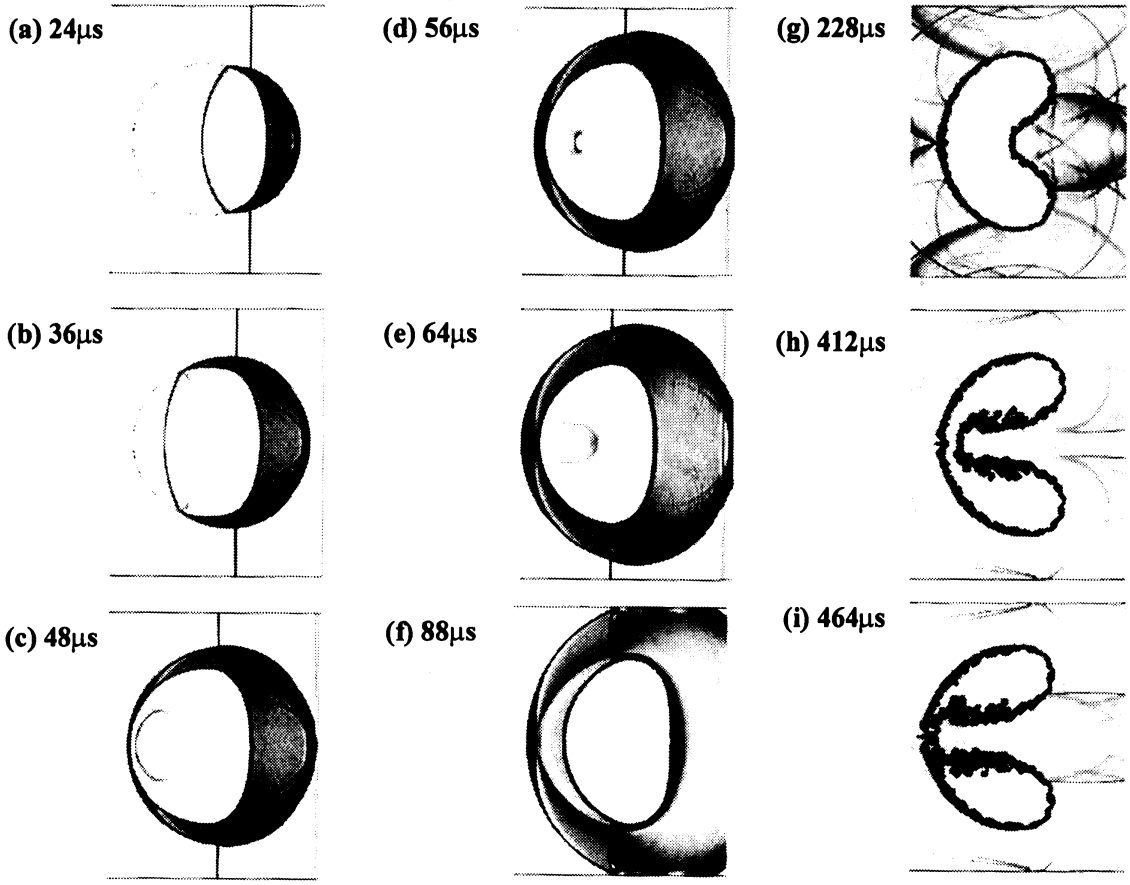

Figure 2. Idealized Schlieren images generated following the methodology outlined in [8] (using the magnitude of the gradient of the density). a) 24 μs, b) 36 μs, c) 48 μs, d) 56 μs, e) 64 μs, f) 88 μs, g) 228 μs, h) 412 μs, i) 464 μs. Times are estimates after the shock impact into the bubble.

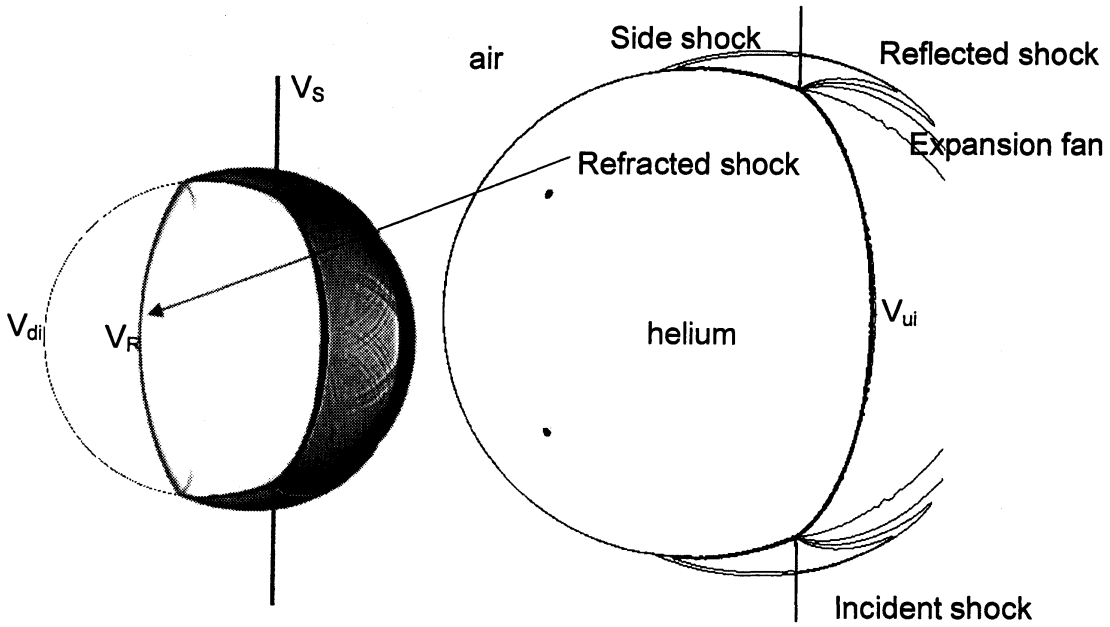

Figure 3. Twin regular reflection-refraction (TRR) shock configuration as well as the locations used to compare the shock waves velocities. V_S : velocity of incident shock. V_R : velocity of refracted shock. V_T : velocity of transmitted shock. V_{ui} : velocity of upstream edge of bubble, initial times. V_{di} : velocity of downstream edge of bubble, initial times. V_j : velocity of jet head.

velocity	Vs	VR	VT	Vui	Vdi	Vj
Haas & Sturtevant (1987, exp.)	410	900	393	170	145	230
Present Computation	418	1080	370	200	141	236
Quick and Karni (1996, comp.)	422	943	377	178	146	227

Table 1. Comparison of shock waves velocities

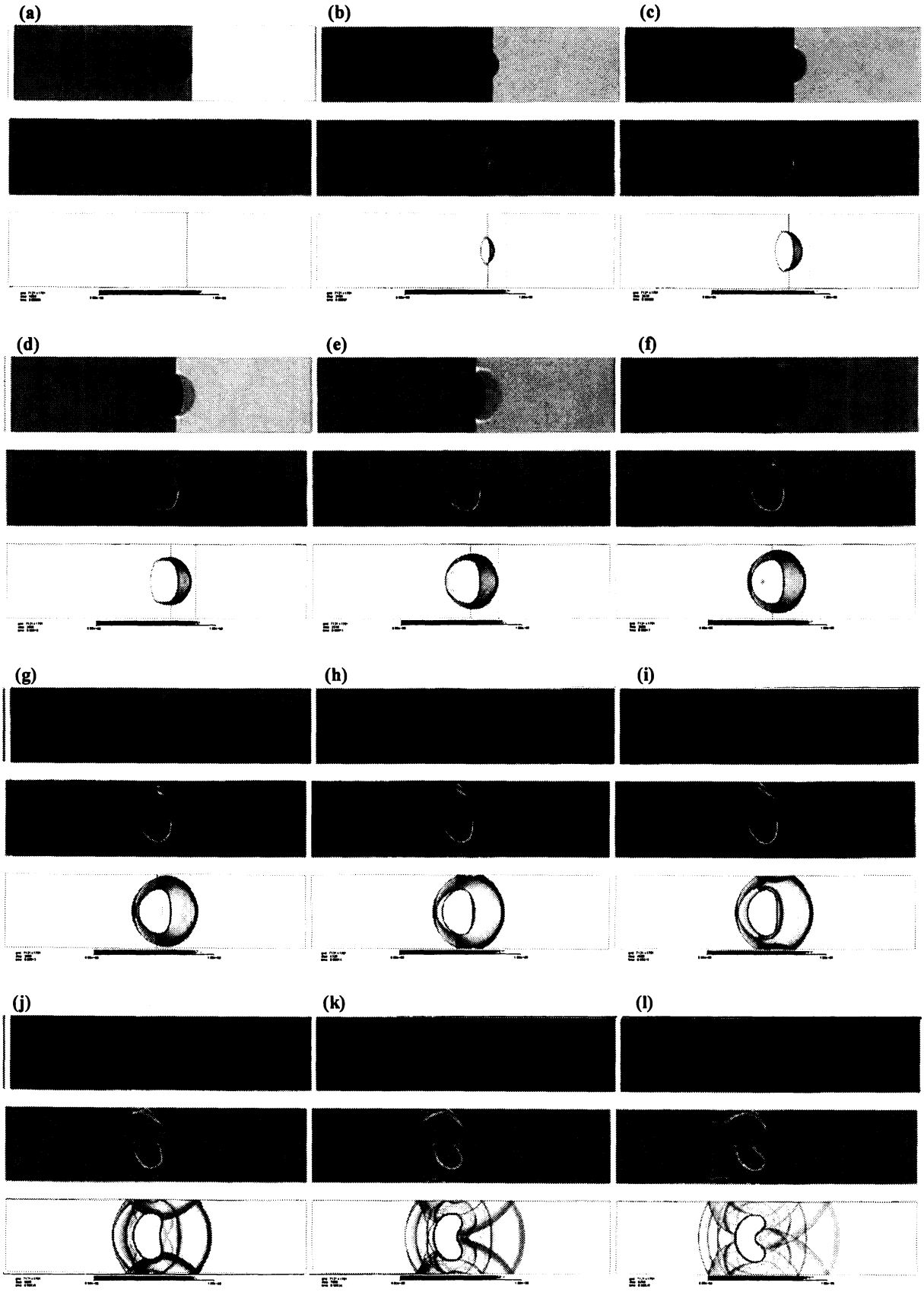

Figure 4 (a-l). For caption see next page.

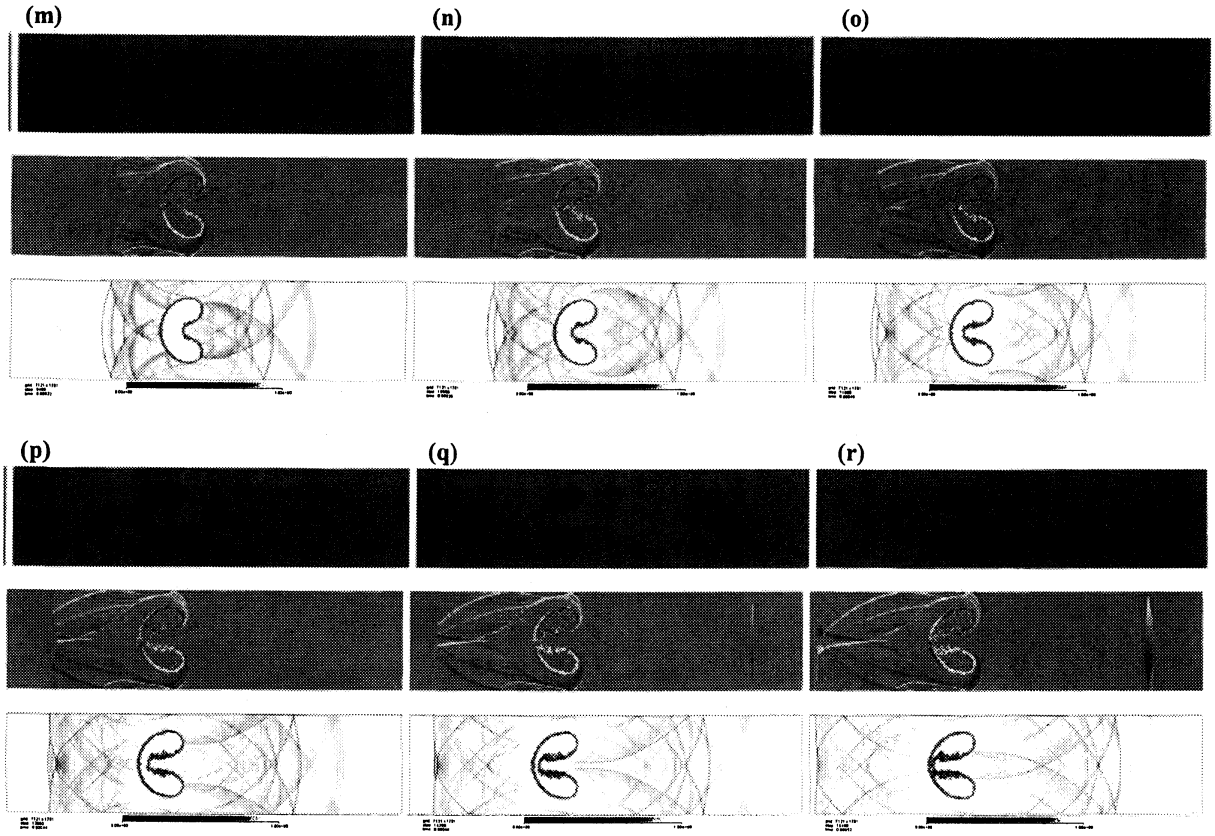

Figure 4. Flow visualization. Density, Vorticity and Density Function.